AD-A039 843 NAVAL RESEARCH LAB WASHINGTON D C F/G 20/14
FOCUSING CHARACTERISTICS OF SYMMETRICALLY CONFIGURED BOOTLACE L--ETC(U)
APR 77 J P SHELTON DOT-FA75WAI-556
UNCLASSIFIED NRL-MR-3483 NL

1 OF 1
AD4039 843

END
DATE
FILMED
6-77

12

NRL Memorandum Report 3483

Focusing Characteristics of Symmetrically Configured Bootlace Lenses

J. P. SHELTON

Microwave and Electromechanical Research Staff
Radar Division

April 1977

NAVAL RESEARCH LABORATORY
Washington, D.C.

SECURITY CLASSIFICATION OF THIS PAGE (When Data Entered)

9

REPORT DOCUMENTATION PAGE

READ INSTRUCTIONS BEFORE COMPLETING FORM

1. REPORT NUMBER: NRL Memorandum Report 3483	2. GOVT ACCESSION NO. 14 NRL-MR-3483
	3. RECIPIENT'S CATALOG NUMBER
4. TITLE (and Subtitle): 6 FOCUSING CHARACTERISTICS OF SYMMETRICALLY CONFIGURED BOOTLACE LENSES.	5. TYPE OF REPORT & PERIOD COVERED: Interim report on a continuing NRL problem.
	6. PERFORMING ORG. REPORT NUMBER
7. AUTHOR(s): 10 J. P. Shelton	8. CONTRACT OR GRANT NUMBER(s)
9. PERFORMING ORGANIZATION NAME AND ADDRESS: Naval Research Laboratory, Washington, D.C. 20375	10. PROGRAM ELEMENT, PROJECT, TASK AREA & WORK UNIT NUMBERS: ~~NRL Problem R12-19~~ 15 DOT-FA75WAI-556
11. CONTROLLING OFFICE NAME AND ADDRESS: DOT/FAA/MLS Office (ARD-720), Washington, D.C. 20362	12. REPORT DATE: 11 April 1977
	13. NUMBER OF PAGES: 12 31 p.
14. MONITORING AGENCY NAME & ADDRESS (if different from Controlling Office)	15. SECURITY CLASS. (of this report): UNCLASSIFIED
	15a. DECLASSIFICATION/DOWNGRADING SCHEDULE

16. DISTRIBUTION STATEMENT (of this Report)

Approved for public release; distribution unlimited.

17. DISTRIBUTION STATEMENT (of the abstract entered in Block 20, if different from Report)

18. SUPPLEMENTARY NOTES

19. KEY WORDS (Continue on reverse side if necessary and identify by block number)

Microwave
Lens
Antenna
Optics

20. ABSTRACT (Continue on reverse side if necessary and identify by block number)

The line-source bootlace lens, invented by Gent in 1956 and analyzed by Rotman and Turner in 1963, produces optimum focusing characteristics when it is constrained to exhibit front-to-back as well as right-left symmetry. It is shown that the symmetric bootlace lens is a one-parameter family when the radiating array is specified to be $\lambda/2$ spaced with ± 90-degree coverage. Design equations for the lens are derived, and overall focusing performance and design data are plotted. A computer program of the design equations is presented.

lambda + or -

251950

CONTENTS

I. INTRODUCTION 1

II. PRELIMINARY CONSIDERATIONS.............................. 4

Performance Parameters 4

The Case for Symmetry 4

III. DESIGN DATA 10

IV. GENERAL DISCUSSION OF BOOTLACE LENSES 14

V. CONCLUSIONS 16

REFERENCES 17

APPENDIX 18

FOCUSING CHARACTERISTICS OF SYMMETRICALLY
CONFIGURED BOOTLACE LENSES*

I. Introduction

The bootlace lens was invented by H. Gent in 1956. [1, 2] As shown in Figure 1, it uses a planar, homogeneous wave-transmission region which has a set of feed ports on one side and a set of lens ports on the other. For the case in which the radiator array is constrained to a straight line, it has been shown that perfect focus can be obtained at three points on the feed curve. [3]

Design equations of the bootlace lens were presented by Rotman and Turner in 1963, and they also gave examples of aberration characteristics. [4] Archer has recently described applications of the lens. [5] Whereas the primary intended application of the lens in the 50's was for rapid mechanical scan by means of feed motion, recent interest has been based on the lens' capabilities as a multiple-beam system. Gent lenses have been used recently in experimental precision aircraft landing systems in Australia and the United States.**[6]

Rotman and Turner required that the feed curve be circular and optimized the design parameters accordingly. This was consistent with rapid mechanical scan of feed horn. In terms of multiple-beam configurations, however, requiring the feed curve to be a circle is an unnecessary constraint. The design study described in this paper placed no limitation on the shape of the feed curve, and concluded that the lens should exhibit front-to-back symmetry. Furthermore, although examples of aberration characteristics were presented by Rotman and Turner, it is not possible to predict lens performance for all cases using their paper. That is, the design limitations of the lens were not established. Sufficient computation has been done to present in this paper a comprehensive description of the focusing characteristics of a symmetrically configured class of these lenses.

This paper does not treat the amplitude distributions produced at the aperture of the lens, nor does it address the far-field pattern characteristics, since these are determined by both the phase and amplitude distributions at the aperture. The analysis is based on geometrical optics ray-tracing techniques.

* The work described in this report was performed under Interagency Agreement DOT-FA75WAI-556 for the Federal Aviation Administration.

** Australia's Interscan Microwave Landing System employs a Gent lens for flare elevation guidance.

Note: Manuscript submitted March 31, 1977.

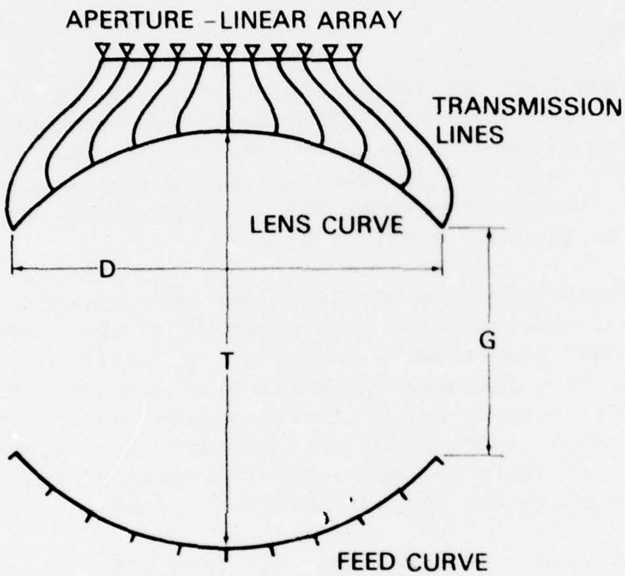

Fig. 1 — Gent lens configuration

The next section of the paper reviews preliminary considerations with regard to performance and design parameters and introduces a symmetry concept. The third section presents design characteristics. The design equations for these lenses are derived in the Appendix, and a listing of a computer program for generating lens dimensions is given.

II. Preliminary Considerations

Performance Parameters

A typical wavefront aberration curve produced by a bootlace lens is sketched in Figure 2. The lens is coma-limited in that the predominant aberration is described by a cubic function. If the maximum wavefront aberration is plotted versus the location on the feed curve, the result is shown in Figure 3. Thus, not only is the dominant aberration cubic, but the magnitude of aberration is also a third-order polynomial in the displacement along the feed or focal curve.

One objective of this section is to define a measure of aberration and a method for determining the portion of the feed curve that yields a given performance level for a particular lens design. A wavefront error surface has been used for this purpose, and a typical surface is depicted in Figure 4. The level of the surface relative to the z_1, z_2 plane represents the amount by which the wavefront, located at aperture point z_2, deviates from ideal linear collimation for any feed point located at z_1. The intersection of the plane, z_1 = constant, with the error surface gives the wavefront error curve for that feed point. Thus, Figure 4 contains a complete description of the focusing performance of the lens. The three foci for the example are at $z_1 = 0$ and $z_1 = \pm 1$. The reference linear wavefronts from which the error surface is computed are chosen so that every error curve has zeros at $z_2 = 0$ and $z_2 = \pm 1$. For lens configurations with right-left symmetry, the error surface is symmetric about the origin. If front-to-back symmetry is imposed, z_1 and z_2 are interchangeable, and the error surface is also symmetric about the lines $z_2 = \pm z_1$. The error surface has four relative extrema, one in each quadrant, and these are labeled δ_1 and δ_2. By symmetry, these extrema are located on the lines $z_2 = \pm z_1$.

To determine the region over which the feed and lens curves are usable, the larger of $|\delta_1|$ or $|\delta_2|$ is selected and called δ_m. Then the maximum values of $|z_2|$ and $|z_1|$, referred to as z_m, are increased until $|\delta_3|$, $|\delta_4|$, $|\delta_5|$ or $|\delta_6| = \delta_m$. δ_3 and δ_6 are the values of the error surface at the four points defined by $|z_1| = |z_2| = z_m$. δ_4 and δ_5 are the local extrema on the intersections of the error surface with the planes defined by $|z_1| = z_m$ and $|z_2| = z_m$. In general, $\delta_3 = \delta_4 = \delta_5 = \delta_6 = 0$ for $z_m = 1$ and the absolute values of δ_3, δ_4, δ_5, δ_6 increase monotonically with increasing z_m. It is found that δ_m is determined by δ_1, and z_m is determined by δ_3 for lenses that are likely to be of practical interest.

The Case for Symmetry

The lens configurations presented in this paper have the symmetry illustrated in Figure 5. The lens and feed curves are identical with opposite orientations. The port locations on the lens and feed curves

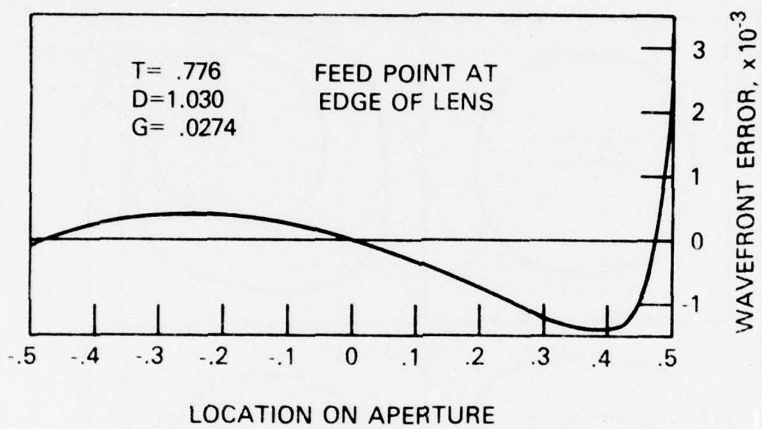

Fig. 2 — Example of wavefront aberration curve (location on aperture)

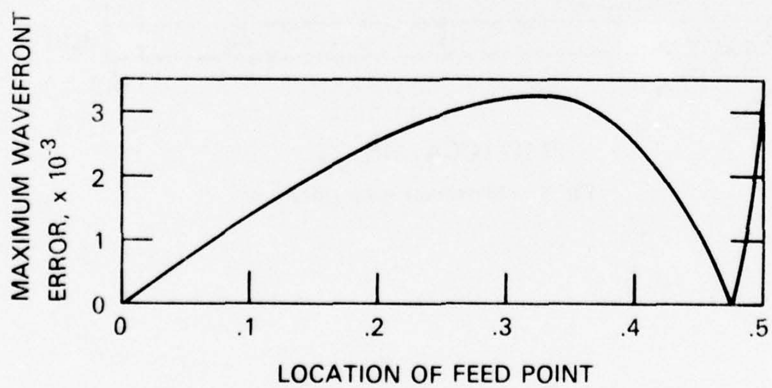

Fig. 3 — Maximum wavefront error vs feed location (location of feed point)

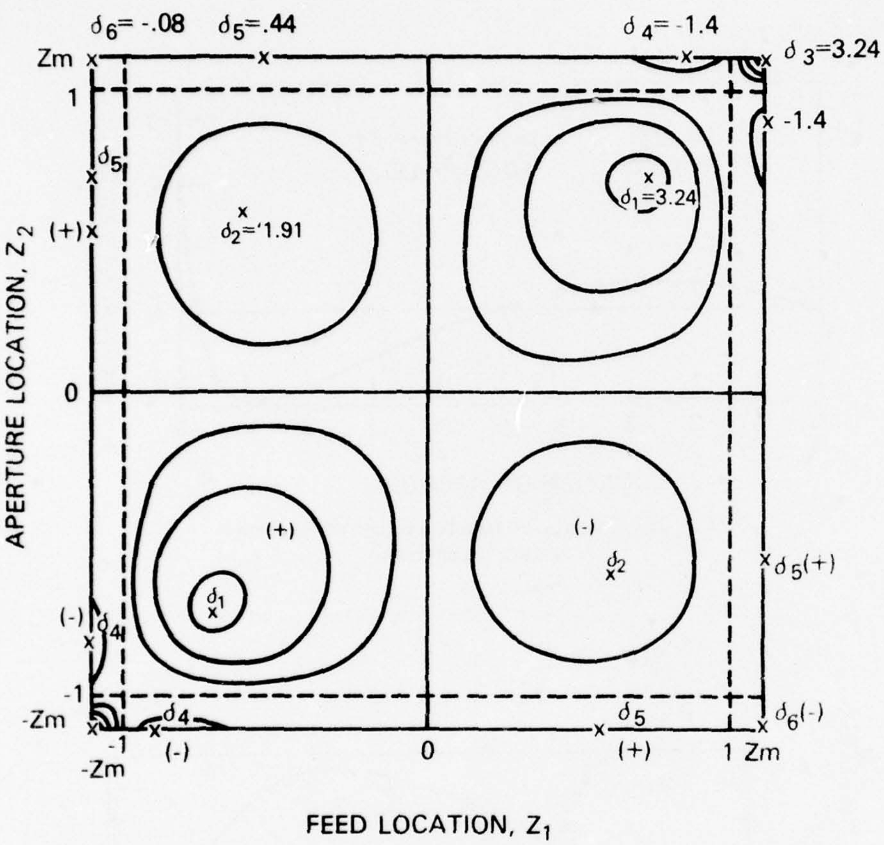

Fig. 4 — Wavefront error surface

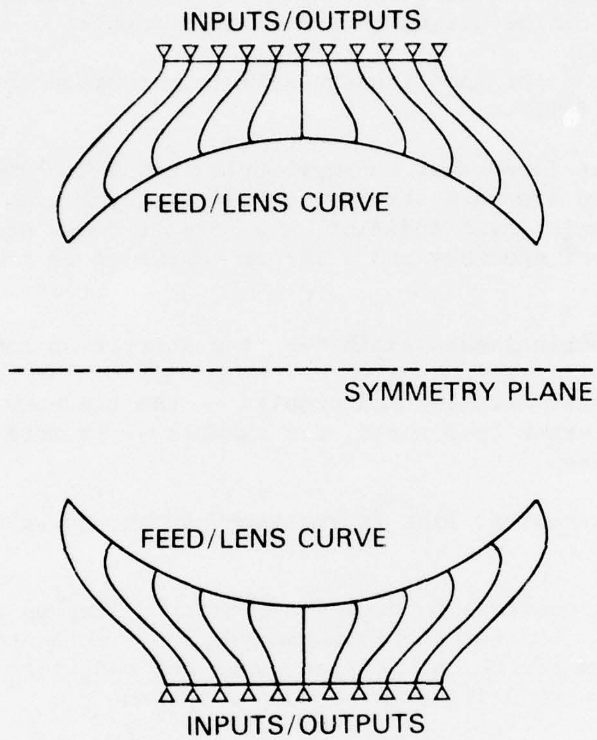

Fig. 5 — Symmetric lens configuration

are also identical. Further, a set of transmission lines is connected to the feed ports, identical with the lines connecting the lens ports with the array elements. The resulting configuration exhibits front-back as well as right-left symmetry, and the input ports and array ports can be interchanged. In the original concept of the bootlace lens, the transmission lines constitute the lens. In the configuration of Figure 5, the lens is compound rather than simple in the optical sense, and it can be viewed as a symmetric doublet.

The reasons for choosing the symmetric configuration are collected and listed as follows:

1. It was found that an asymmetric lens will have either the lens arc or the feed arc more strongly curved than the arcs obtained for the symmetric solution. In addition, the more strongly curved arc will have larger port spacings and a larger variation in port spacing from center to edge.

2. Symmetric lenses exhibit better aberration characteristics.

3. The self-illumination problem -- the tendency for feed ports to illuminate other feed ports, for example -- is more severe for asymmetric lenses.

4. The symmetric lens is smaller than an equivalent asymmetric lens.

5. It is possible to divide a symmetric lens on its line of symmetry with a reflecting plane and realize a reflection-type collimating system for which the feed ports and radiating ports are identical. Figure 6 illustrates such a system.

6. If some type of beam synthesis is to be carried out using combinations of beams, the symmetric configuration with two sets of transmission lines must be used to insure that all beams have the same far-field phase reference. The formation of monopulse patterns is an example of such synthesis.

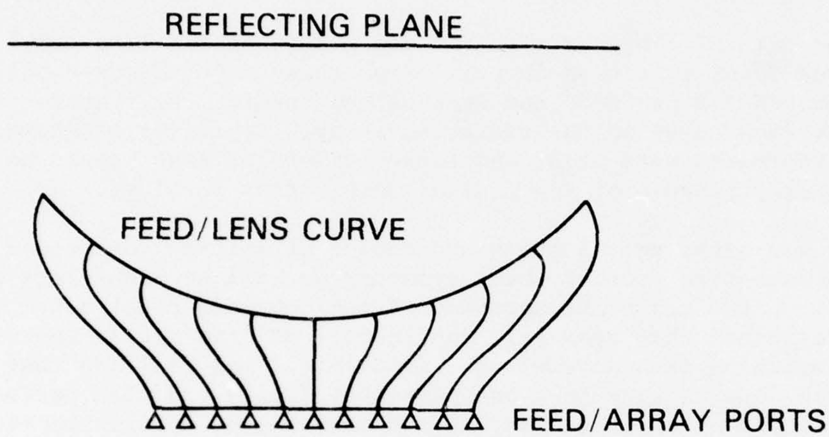

Fig. 6 — Reflection type lens configuration

III. Design Data

The derivation of these design equations for Gent lenses followed a not uncommon course for exploratory analysis -- the initial objectives were not achieved by the final results. The initial objective was to derive a simplified design procedure without regard to symmetry. The purpose was to obtain general relationships about the lenses rather than detailed design information.

The initial analysis used the end points of the lens curve and the three focal points as inputs. From these, fourth power polynomials were derived for the feed and lens curves and for the transfer function from the lens curve to the radiating array. Approximate estimates of lens performance were made, and large numbers of cases could be tested very quickly because of the minimal computation involved.

It was noted that a judicious choice of initial conditions produced a lens with front-to-back symmetry as well as right-left symmetry, at least to the six place accuracy of the computer print-out. Then it was ascertained that symmetric configurations give better aberration characteristics than asymmetric. Finally, it was realized that the symmetric lens represents a one-parameter family and that performance evaluation on an exact basis could be carried out straightforwardly. At this point the approximate analysis was abandoned, and the exact solution for the symmetric lens, outlined in the Appendix, was derived.

The design equations derived in the Appendix have been programmed for computer calculation, and some of the results are plotted in Figure 7. The basic parameters of interest -- lens dimensions normalized to aperture length, element spacings relative to $\lambda/2$, and maximum wavefront deviation relative to the aperture length -- are presented in terms of lens thickness, T. Figure 8 is a plot of the lens shapes for T = .775, 1.04 and 1.65. It is not accidental that the endpoints of the lens curves shown in Figure 8 appear to fall on a straight line. It is shown in the Appendix that $T-G \approx .75$, and it has been found that actual design data deviate by less than .002. Thus, the axial depth of lens and feed curves, which is $(T-G)/2$, is very nearly 3/8 the aperture length for all lenses.

As described in the Appendix, the symmetric Gent lens forms a one-parameter family, and this parameter can be any one of the dimensions plotted in Figure 7. The dimensionless parameter A is also plotted because the design equations use A (or C) as one of the initial inputs. All lenses have been scaled so as to provide ± 90 degrees coverage from a radiating array of half wavelength spaced elements.

It is notable that the wavefront deviation is a rapidly varying function of lens size. Doubling the lens thickness reduces aberration by a factor of ten. If the allowable wavefront deviation is $\pm\lambda/16$, it is found that the most compact lens -- with T = .78 -- is usable with

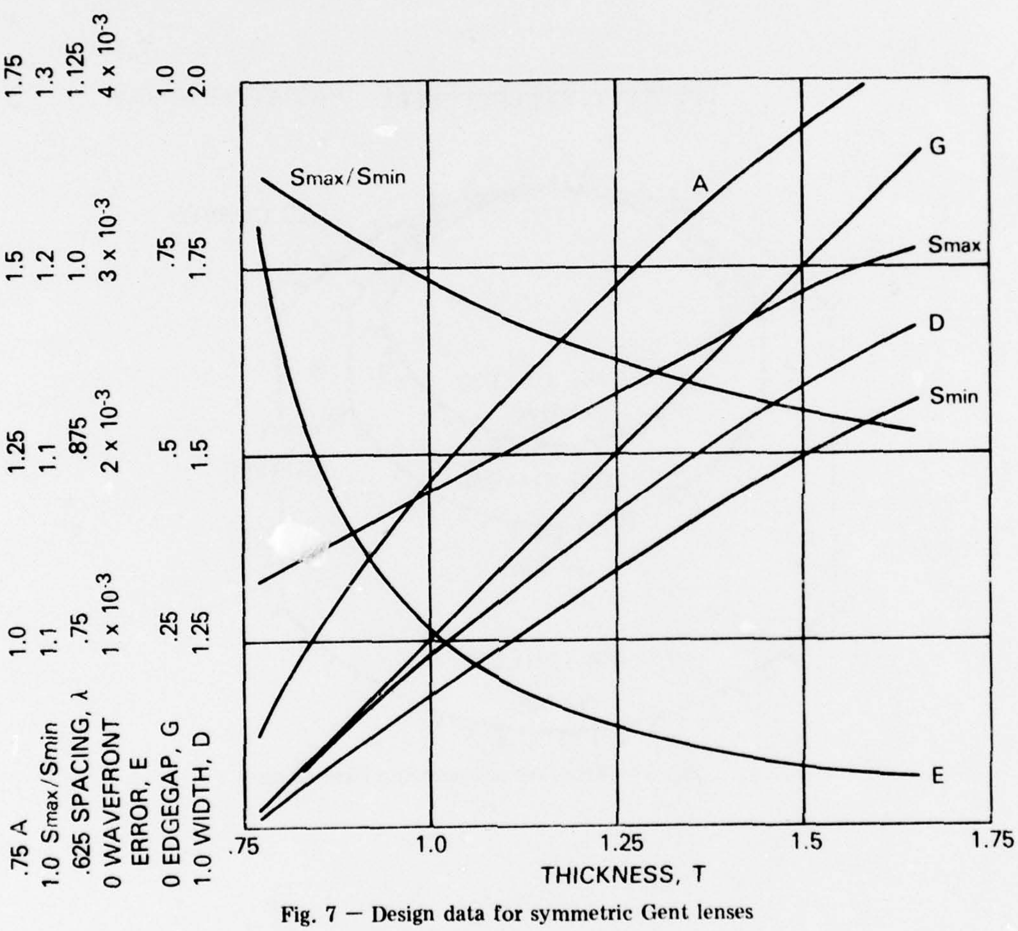

Fig. 7 — Design data for symmetric Gent lenses

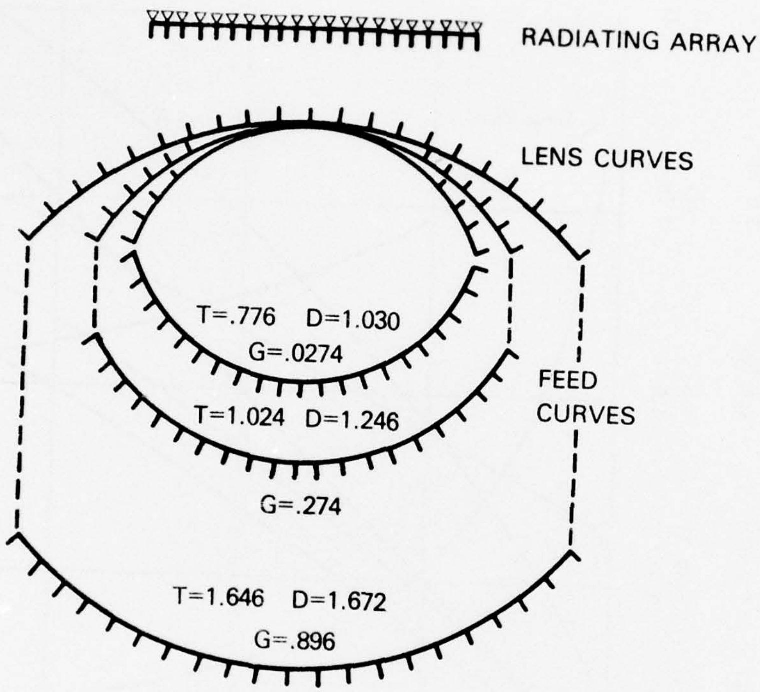

Fig. 8 — Examples of symmetric Gent lenses

a maximum aperture size of 20λ. A lens of intermediate compactness, with T = 1, is usable with an aperture as large as 60λ. For T = 1.5, the aperture can be 180λ.

Many optical systems have aberration which is a power of some parameter such as the F/D ratio. The availability of such a relationship simplifies the analysis of the optical system in practical applications. An attempt was made to deduce a simple functional relationship between wavefront deviation and one of the lens parameters, but regrettably without success.

The element spacings on the feed and lens curves are consistent with phased array theory applied to arrays with limited angular coverage. [7] An efficient linear phased array radiator with ideally suited directive characteristics and coverage limits of θ_1 and θ_2 will have elements spaced according to

$$s = \frac{\lambda}{\sin \theta_2 - \sin \theta_1} .$$

For the most compact lens, with G=0, T=3/4, and D=1, the center elements have $\theta_2 = \tan^{-1}\frac{4}{3}$ and $\theta_1 = -\tan^{-1}\frac{4}{3}$, giving $s_{min} = .625\lambda$. The edge elements have $\theta_2 = \tan^{-1}3$ and $\theta_1 = -\tan^{-1}\frac{1}{3}$, giving $s_{max} = .7906\lambda$. These values are seen to be close to the limiting values as $T \rightarrow .75$, of the s_{min} and s_{max} curves in Figure 7.

In order to obtain specific design information to be used in constructing a lens, one must use the equations presented in the Appendix. Figure A-1 of the Appendix should be examined at this point and the dimensional parameters defined thereon understood. Figure 7 is useful in predicting the general dimensions and performance of a particular lens. The procedure is to select a candidate lens from Figure 7, determine the appropriate value of the parameter A, and then enter the design equations at Equation (A-7). Alternatively, one may use the computer program, using the number of ports and the value of A as inputs.

IV. General Discussion of Bootlace Lenses

Although the primary purpose of this paper is to present theoretical design data for bootlace lenses, it is also worthwhile to examine the more general comparison between the characteristics of these lenses and "ideal" bootlace lenses. A listing of the actual and ideal characteristics is presented in Table I.

Table I. Comparison of Actual & Ideal Lens Characteristics

Design Feature	Actual Lens	Ideal Lens
1. Interconnecting transmission lines	Lines have variable lengths	All lines should have equal length
2. Feed & lens curves	Both curves have strong curvature	Both curves should be straight lines
3. Required port radiation patterns	Patterns become asymmetric for off-axis ports	Patterns should be symmetric for all ports
4. Port spacing function	Port-spacing increases for off-axis ports	Port spacing should be constant for all ports
5. Output amplitude distribution	Becomes asymmetric for off-axis ports	Should be uniform or at least symmetric for all ports

Table I indicates that the conventional bootlace lens, although it is quite good, is far from ideal. It can be shown that items 1 and 3 are directly related. That is, if a lens can be devised with all line lengths equal, it will automatically require symmetric port radiation patterns. It can also be shown that if item 4 is satisfied, the lens can radiate directly without using the lens or radiator arrays or the interconnecting lines. That is, if item 4 is satisfied, the lens is no longer of the bootlace type. Thus, for bootlace lenses, Table I can be reduced to three design features for comparing actual and ideal lenses--interconnecting line lengths, feed and lens curves, and amplitude distribution. J. P. Wild has proposed an ingenious bootlace lens configuration which satisfies the ideal requirements for these design features. [8] The parallel-plate portion of the lens is not a planar surface, however.

No mention has been made of the focal length of these lenses, nor of other optical parameters such as field of view. Rotman and Turner used such terms, defining focal length as the center-line length of the wave transmission region and equating the angle to the off-axis focus to the coverage by requiring that the port spacing of the radiating array be equal to that at the center of the lens curve.

The design procedure of this paper emphasizes internal consistency in terms of array theory. The resultant lens-antenna system has a half-wave spaced array of N radiators fed by an N-port lens. The N beams will just cover the ± 90 deg of visible space. Note that lenses defined in this way have performance equivalent to that of a Butler matrix. If we desire to obtain M beams from an N-element array, where M<N, we do not utilize a smaller portion of the feed curve of an N-beam lens. Instead, we elect to fill the lens curve of an M-beam lens with N elements. Therefore, all lens configurations are symmetric, whether N x N (elements x beams) or N x M. This design rule has the effect of greatly reducing the complexity of the design process.

It may be somewhat disturbing to realize that the N x M configuration may result in arbitrarily small port spacings for the lens curve. Although this may present some practical difficulty, it is theoretically plausible. The lens ports will be mutually coupled and mismatched for small port spacings. However, the feed ports will be matched and the lens will be theoretically lossless as seen from the feed ports. This is analogous to the extreme case of obtaining a single beam from an array using a power divider. The power divider is mismatched when viewed from a single array port. Furthermore, a multibeam antenna array should ideally have one radiator for each beam, even for small overall angular coverage. [9] In a practical realization, careful engineering design should always yield $M \geq N/2$, or no more than two radiators per beam. Thus, the minimum element spacing on the lens curve will be about $.3\lambda$ to $.4\lambda$.

V. Conclusions

The focusing performance of a symmetric class of line-source, multiple-beam bootlace lenses has been evaluated. Design data for the lenses have been presented in graphical form. Design equations and a computer program for generating detailed lens dimensions have also been presented. All designs have been normalized to produce ± 90-degree coverage from a $\lambda/2$ spaced array of radiators. It is found that the most compact lens, with width about equal to the length of the array and thickness of .75 times the length of the array, can feed an aperture of 20λ or about 40 elements. Increasing the size of the lens relative to the radiating array sharply reduces the wavefront aberration; doubling the thickness of the lens reduces aberration by a factor of ten, making apertures of 200λ feasible.

REFERENCES

1. H. Gent, "The Bootlace Aerial," Royal Radar Establishment Journal, pp. 47-57, October 1957.

2. S.S.D. Jones, H. Gent, and A.A.L. Browne, "Improvements in or Relating to Electromagnetic-Wave Lens and Mirror Systems," British Provisional Patent Specification No. 25926/56; August 1956.

3. M. L. Kales and R. M. Brown, "Two-Dimensional Symmetric Bootlace Lenses," IEEE Trans., Vol. AP-13, pp. 521-528, July 1965.

4. W. Rotman and R. F. Turner, "Wide-Angle Microwave Lens for Line Source Applications," IEEE Trans., Vol. AP-11, No. 6, pp. 623-632, November 1963.

5. D. Archer, "Lens-Fed Multiple-Beam Arrays," Microwave Journal, Vol. 18, No. 10, pp. 37-42, Oct. 1975.

6. R. M. Cox and J. R. Sebring, "MLS--A Practical Application of Microwave Technology," IEEE Trans., Vol. MTT-24, No. 12, pp. 964-971, Dec., 1976.

7. W. K. Kahn, "Ideal Efficiency of a Radiating Element in an Infinite Array," Trans. IEEE, Vol. AP-15, pp. 534-538, July, 1967.

8. J. P. Wild, Radiophysics Laboratory, CSIRO, Sydney, Australia, private communication.

9. R. S. Mailloux, "An Overlapped Subarray for Limited Scan Application," Trans. IEEE, Vol. AP-22, No. 3, pp. 487-489, May 1974.

Appendix

Derivation of Lens Design Equations

The initial configuration is shown in Figure A-1. The lens curve, plotted in an x-y plane, is specified by the points (0,0) and ($\pm$1, A-C). The foci are at (0, 2A-C) and ($\pm$1,A). These six points are chosen so that the lens exhibits the desired symmetry. The corresponding portion of the radiating aperture covers the interval $-1 < z < 1$. Pathlengths from the foci to arbitrary lens curve locations (x, y), thence through the transmission lines L to the radiating aperture at z are indicated. The following guarantee the collimation of wavefronts from the three foci:

$$L(x, y) = L = \ell_1 - \ell_2$$
$$= 2A - C - \ell_2 \qquad \text{(A-1)}$$

Equation (A-1) collimates all rays from F_o.

$$\ell_4 + L = \ell_3 - kz/2 \qquad \text{(A-2)}$$

$$\ell_5 + L = \ell_3 + kz/2 \qquad \text{(A-3)}$$

Equations (A-2) and (A-3) collimate all rays from F_1 and F_2. The constant k must be determined.

Expressions for the pathlengths are as follows:

$$\ell_3 = \sqrt{A^2 + 1}$$

$$\ell_4 = \sqrt{(x - 1)^2 + (A - y)^2}$$

$$\ell_5 = \sqrt{(x + 1)^2 + (A - y)^2}$$

$$\ell_2 = \sqrt{x^2 + (2A - C - y)^2}$$

Equations (A-2) and (A-3) become

$$\sqrt{(x + 1)^2 + (A - y)^2} - \sqrt{(x -1)^2 + (A - y)^2} = (\sqrt{C^2 + 4} - C)\, z \qquad \text{(A-4)}$$

$$\sqrt{(x + 1)^2 + (A - y)^2} + \sqrt{(x -1)^2 + (A - y)^2} = 2(\sqrt{A^2 + 1} - 2A + C +$$
$$\sqrt{x^2 + (2A - C - y)^2}) \qquad \text{(A-5)}$$

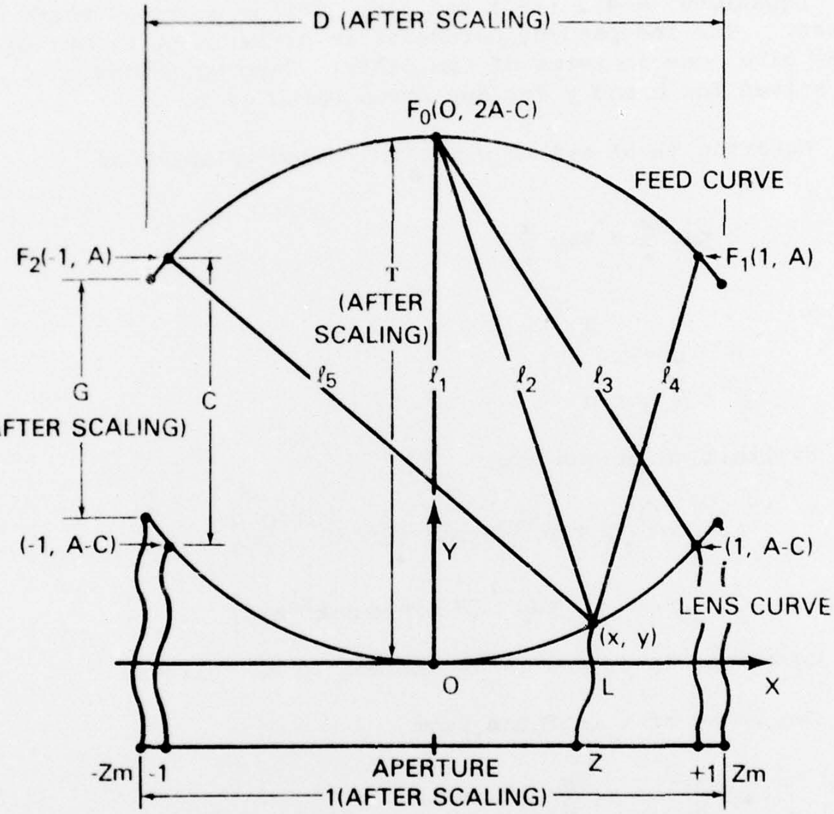

Fig. A-1 — Lens geometry used for design equations where $k = \sqrt{C^2 + 4} - C$ since $x = 1$, $y = A - C$, $z = 1$ is an initial constraint. This same constraint applied to Equation (A-5) yields

$$4(\sqrt{A^2 + 1} - A) = \sqrt{C^2 + 4} - C \tag{A-6}$$

Equations (A-4), (A-5) and (A-6) define a one-parameter family of lenses. The independent parameter is either A or C, and Equation (A-6) gives one in terms of the other. Then Equations (A-4) and (A-5) are solved for x and y for any given value of z.

Equation (A-6) can be expressed parametrically as

$$2 \tan \frac{w}{2} = \tan \frac{u}{2} ,$$

where

$$A = \cot w$$

$$C = 2 \cot u$$

Explicit solutions are

$$A = \cot \left\{ 2 \tan^{-1} [\tfrac{1}{2} \tan (\tfrac{1}{2} \cot^{-1} \tfrac{C}{2})] \right\}$$

$$C = 2 \cot \left\{ 2 \tan^{-1} [2 \tan(\tfrac{1}{2} \cot^{-1} A)] \right\} \tag{A-7}$$

Equations (A-4) and (A-5) are solved as follows:

The value of x is found from

$$a(\frac{2x}{U})^2 + b(\frac{2x}{U}) + c = 0,$$

taking the positive value of the root,

where

$$a = 4 - U^2 - \frac{V^2}{(A - C)^2}$$

$$b = \frac{4WV}{(A - C)^2}$$

$$c = U^2 - 4 - \frac{4W^2}{(A - C)^2}$$

$$W = \frac{V^2 - U^2}{8} + \frac{1 - (A - C)^2}{2}$$

$$U = z(\sqrt{4 + C^2} - C)$$

$$V = 2(-2A + C + \sqrt{A^2 + 1})$$

The value of L is given by

$$L = 2A - C - \sqrt{x^2 + (2A - C - y)^2}$$

The next step in the design procedure is to determine the extent of the lens and feed curves that can be used to provide the best possible performance from the lens. As indicated in Figure 4, a maximum wavefront deviation, δ_m, is found on the interfocal region of the feed curve. Then the maximum usable value of z is found by trying values of $z > 1$ until the wavefront deviation equals δ_m. It was found that z_m is a function of A, and Figure A-2 is a plot of this relationship. If the wavefront error function were exactly cubic in terms of z, then z_m would be $2/\sqrt{3}$, or 1.1547. For $A = 10$, $z_m = 1.1500$, which supports the hypothesis that $z_m = 1.1547$ is an asymptote of the curve of Figure A-2. Figure A-3 is a plot of the quantities, δ_n/δ_m, for $n = 1$ to 6, as a function of A. Figure A-3 shows clearly the variation of the error surface from the ideal cubic function for small A. The surface becomes more nearly cubic as A increases. If Figure A-3 were extended to $A = 10$, it would be found that all values of δ_n/δ_m exceed .86.

Once the value of z_m is determined for given A, it is possible to obtain lens dimensions for a radiating array of any number of elements by uniformly spacing the elements between $-z_m$ and z_m and solving for x, y, and L.

The above design equations generated lenses that are "unscaled", so called because the scale factor relating the lens size and the radiating array size was arbitrarily chosen. In order to best meet the needs of the design engineer, a scaling procedure is applied so that the edge feed position produces an end-fire beam from the array. Furthermore, the aperture length is given a value of unity, so that all dimensions are normalized in terms of the aperture. Methods for obtaining coverage other than ± 90 degrees from the lens-array combination are discussed in Section IV. A scale factor of

$$g = \frac{1}{[\ell_3(z_m) - \ell_1(z_m)]z_m}$$

is multiplied by all values of x, y, L, and δ to describe the scaled lens dimensions. For the unscaled lens, the edge feed position, with $z=z_m$, produces a beam which makes an angle relative to the array normal given by $\sin\theta_m = [\ell_3(z_m) - \ell_1(z_m)]/2$, where $\ell_3(z_m)$ and $\ell_1(z_m)$ are

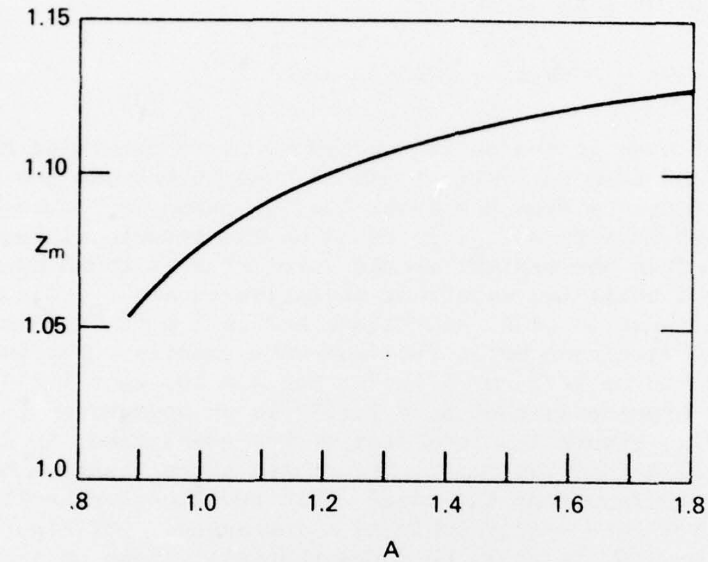

Fig. A-2 — Z_m vs A

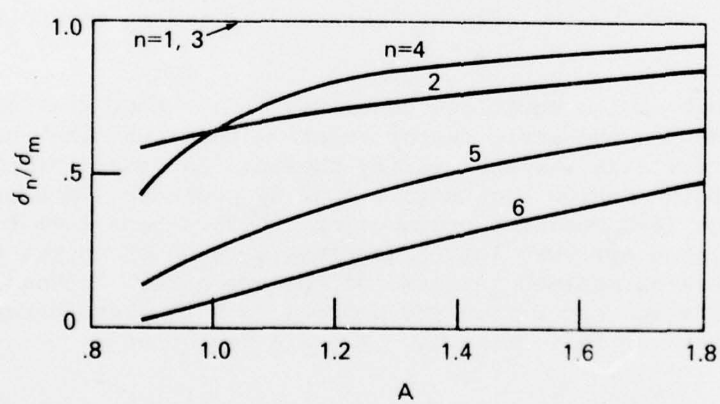

Fig. A-3 — δ_n/δ_m vs A

pathlengths from the edge of the feed curve to $x = \pm 1$ on the lens curve. In order to make $\theta_m = 90$ deg. we multiply the lens dimensions by $2/[\ell_3(z_m) - \ell_1(z_m)]$. Then, in order to normalize all dimensions to an aperture of unity, we divide by $2z_m$.

It is possible to obtain approximate relationships for the scaled lenses by assuming that $z_m = 1$ and applying the scaling factor. It is then found that

$$T = \frac{D^2}{2} + \tfrac{1}{4}$$

$$T = G + 3/4,$$

where T is the lens thickness or spacing between center points of the lens and feed curves, D is the lens width, and G is the edge gap or minimum spacing between lens and feed curves. The smallest lens is obtained for $G = 0$, $T = 3/4$, and $D = 1$.

These design equations, starting with Equation (A-7), have been programmed in BASIC language. The program generates the following outputs:

1. Unscaled wavefront errors for the surface of Figure 4, for $z_1 = \pm z_2$ and $z_1 = z_m$.

2. Scaled dimensions for the lens and feed curves.

3. Transmission line lengths.

4. Ratio of lens element spacing to array element spacing.

5. Overall lens dimensions relative to array -- thickness, width, and edge gap.

6. Maximum wavefront error for scaled lens.

Input data to the program are A and J, where the number of elements in the array and feeds to the lens are 2J + 1. Table A-1 is a listing of the program. Table A-2 is a typical printout for A = .91, J = 20.

Table A-1
Listing of Lens Design Program

```
100  DIM X(60),Y(60),D1(60),D2(60),L(30),S(50)
110  DATA 20
120  DATA .91
125  READ J
130  READ A
135  C=2/TAN(2*ATN(2*TAN(.5*ATN(1/A))))
137  PRINT "A="A,"C="C
140  F=SQR(4+C*C)-C
150  V=2*(-2*A+C+SQR(1+A*A))
160  V2=V*V
170  A2=(A-C)**2
180  Q=0
190  Z1=.55
200  Z2=.7
210  Z3=.01
220  D3=0
230  FOR Z=Z1 TO Z2 STEP Z3
240  GOSUB 1200
250  IF ABS(D1)<ABS(D2) THEN 280
260  D=ABS(D1)
270  GO TO 290
280  D=ABS(D2)
290  IF D>D3 THEN 310
300  GO TO 330
310  D3=D
320  NEXT Z
330  IF (D3-D)/D3<1E-5 THEN 390
340  Z1=Z-2*Z3
350  Z2=Z
355  Z3=Z3/10
360  Q=Q+1
370  IF Q=6  THEN 390
380  GO TO 220
390  Z4=Z
400  PRINT "D="D,"Z="Z
410  Z1=1.05
420  Z2=1.2
430  Z3=.01
440  Q=0
450  FOR Z=Z1 TO Z2 STEP Z3
460  GOSUB 1200
470  IF ABS(D1)<ABS(D2) THEN 500
480  D3=ABS(D1)
490  GO TO 510
500  D3=ABS(D2)
510  IF D3>D THEN 530
520  NEXT Z
```

```
530  Z2=Z
540  Z1=Z-Z3
550  Z3=Z3/10
560  Q=Q+1
570  IF Q=6 THEN 590
580  GO TO 450
590  Z5=Z
600  PRINT "ZMAX="Z
610  PRINT "WAVEFRONT ERRORS FOR INTERNAL PORTS"
620  PRINT "Z","D1","D2"
630  FOR I=1 TO J
640  Z=I*Z5/J
650  GOSUB 1200
660  X(I)=X
670  Y(I)=Y
680  D1(I)=D1
690  D2(I)=D2
700  L(I)=L
710  IF I>1 THEN 740
720  S(I)=SQR(X*X+Y*Y)
730  GO TO 750
740  S(I)=SQR((X-X(I-1))**2+(Y-Y(I-1))**2)
750  PRINT Z,D1,-D2
760  NEXT I
770  PRINT "WAVEFRONT ERRORS FOR EDGE PORT"
780  PRINT "I","D1","D2"
790  FOR I=1 TO J
800  Z=I*Z5/J
810  L4=SQR((2*A-C-Y(J)-Y(I))**2+(X(J)-X(I))**2)
820  L5=SQR(L4**2+4*X(J)*X(I))
830  D1=L2-L4-L(I)-(L3-L1)*Z/2
840  D2=D1+L5+L4+2*(L(I)-L2)
850  PRINT I,D1,-D2
860  NEXT I
870  PRINT "SCALED DIMENSIONS"
880  PRINT "X","Y","L","SPACING RATIO"
890  K=1/((L3-L1)*Z5)
900  FORI=1 TO J
910  X(I)=K*X(I)
920  Y(I)=K*Y(I)
930  L(I)=K*L(I)
940  S(I)=K*S(I)
950  PRINT X(I),Y(I),L(I),2*J*S(I)
960  NEXT I
```

```
970  T=(2*A-C)*K
980  PRINT "THICKNESS="T
990  PRINT "WIDTH="2*X(J)
1000  PRINT "EDGE GAP="T-2*Y(J)
1010  PRINT "WAVEFRONT ERROR/APERTURE="D*K
1015  PRINT
1016  PRINT
1020  GO TO 130
1200  U=F*Z
1210  U2=U*U
1220  W=(V2-U2)/8+(1-A2)/2
1230  B1=4-U2-V2/A2
1240  B2=4*W*V/A2
1250  B3=U2-4-4*W*W/A2
1260  X=(U/4)*(-B2+SQR(B2*B2-4*B1*B3))/B1
1270  Y=A-(W-V*X/U)/(A-C)
1280  L1=SQR((X-1)**2+(A-Y)**2)
1290  L2=SQR(X*X+(2*A-C-Y)**2)
1300  L3=SQR((X+1)**2+(A-Y)**2)
1310  L4=2*A-C-2*Y
1320  L5=SQR(L4*L4+4*X*X)
1330  L=2*A-C-L2
1340  D1=L2-L4-L-(L3-L1)*Z/2
1350  D2=D1+L5+L4+2*(L-L2)
1360  RETURN
2000  END
```

Table A-2

Sample Print-Out of Lens Design Program

```
A= .91             C= .246891
D= 5.69014E-3      Z= .676
ZMAX= 1.0606
```

WAVEFRONT ERRORS FOR INTERNAL PORTS

Z	D1	D2
5.30299E-2	6.80822E-5	-6.78612E-5
.10606	2.70020E-4	-2.66524E-4
.15909	5.98859E-4	-5.81505E-4
.21212	1.04291E-3	-9.99541E-4
.26515	1.58560E-3	-1.45999E-3
.31818	2.20527E-3	-1.95609E-3
.371209	2.87493E-3	-2.43797E-3
.424239	3.56191E-3	-2.86425E-3
.477269	4.22757E-3	-3.19508E-3
.530299	4.82694E-3	-3.39497E-3
.583329	5.30351E-3	-3.43596E-3
.636359	5.61430E-3	-3.30082E-3
.689389	5.68063E-3	-2.98659E-3
.742419	5.44056E-3	-2.50888E-3
.795449	4.83027E-3	-1.90499E-3
.848479	3.80554E-3	-.00124
.901509	2.38665E-3	-6.10468E-4
.954539	7.99081E-4	-1.47408E-4
1.00757	3.87944E-5	-4.35036E-6
1.0606	5.69017E-3	-2.22479E-4

WAVEFRONT ERRORS FOR EDGE PORT

I	D1	D2
1	-1.76745E-4	1.64290E-4
2	-3.65106E-4	3.15394E-4
3	-5.64164E-4	4.52343E-4
4	-7.72883E-4	5.74614E-4
5	-9.90056E-4	6.81306E-4
6	-1.21423E-3	7.71631E-4
7	-1.44361E-3	8.44735E-4
8	-1.67589E-3	8.99703E-4
9	-1.90805E-3	9.35544E-4
10	-2.13602E-3	9.51179E-4
11	-2.35409E-3	9.45422E-4
12	-2.55406E-3	9.16956E-4
13	-2.72363E-3	8.64372E-4
14	-2.84353E-3	7.89070E-4
15	-2.88185E-3	6.80398E-4
16	-2.78193E-3	5.45993E-4
17	-2.43320E-3	3.90720E-4
18	-1.59986E-3	1.85873E-4
19	4.07942E-4	-3.16145E-5
20	5.69017E-3	-2.22479E-4

SCALED DIMENSIONS

X	Y	L	SPACING RATIO
3.18571E-2	9.29943E-4	2.86828E-4	1.27482
6.36333E-2	3.71606E-3	1.14819E-3	1.27593
9.52477E-2	8.36223E-3	2.53570E-3	1.27814
.126618	1.48689E-2	4.60677E-3	1.28152
.157661	2.32382E-2	7.21464E-3	1.28606
.188292	3.34728E-2	1.04185E-2	1.29193
.218424	4.55762E-2	1.42235E-2	1.29886
.247966	5.95523E-2	.018657	1.30726
.276826	7.54062E-2	2.27185E-2	1.31711
.304906	9.31433E-2	.02943	1.32853
.332106	.11277	3.58109E-2	1.34157
.358319	.134294	4.29971E-2	1.35669
.383432	.157724	5.06703E-2	1.37381
.407329	.183066	5.91984E-2	1.39331
.429888	.21033	6.84912E-2	1.4155
.45099	.239522	7.85651E-2	1.44079
.470531	.270638	8.94136E-2	1.46971
.488473	.30355	.100949	1.50292
.505055	.338433	.112793	1.54133
.522207	.374285	.122854	1.58974

THICKNESS= .790867

WIDTH= 1.04441

EDGE GAP= .042297

WAVEFRONT ERROR/APERTURE= 2.86067E-2